JOURNAL OF CATALYSIS **159,** 58–68 (1996)
ARTICLE NO. 0064

Acidic Properties of Silica-Containing Mixed Oxide Aerogels: Preparation and Characterization of Zirconia–Silica and Comparison to Titania–Silica

James B. Miller and Edmond I. Ko[1]

Department of Chemical Engineering, Carnegie Mellon University, Pittsburgh, Pennsylvania 15213-3890

Received March 23, 1995; revised September 26, 1995; accepted October 23, 1995

In this work we describe our preparation and characterization of zirconia–silica aerogels having 2 : 1, 1 : 1, and 1 : 2 Zr : Si atomic ratios. By preparing samples both with and without silicon precursor prehydrolysis, we also probe different extents of component mixing. Prehydrolyzed samples display improved molecular-scale homogeneity at all compositions as evidenced by total acid site densities, fractional Brønsted populations, and 1-butene isomerization activities that are higher than in corresponding nonprehydrolyzed materials. Acid site densities of our zirconia–silicas are among the highest reported in the literature for comparable materials prepared by a number of different methods, suggesting that the aerogel preparation delivers samples that, even in its nonprehydrolyzed variant, are among the most homogeneously mixed. The effects of prehydrolysis on the catalytic properties of zirconia–silica parallel those we previously reported for titania–silica, illustrating the general applicability of the technique for preparation of well-mixed, two-component oxides. We do, however, observe some important differences between the two oxide pairs. Zirconia–silica is a more active 1-butene isomerization catalyst than titania–silica and, as a function of composition, its maximum activity occurs at a higher silica content (50 mol% silica vs 33 mol%). Within the framework of the Tanabe model of mixed oxide acidity, we explain these observations in terms of the number and transition metal coordination of the Si–O–*M* (*M* = Ti, Zr) linkages accessible in each mixed oxide pair.

INTRODUCTION

Mixed Oxides and the Role of Homogeneity

Important textural, structural, and catalytic properties of mixed oxides depend on the intimacy of molecular-scale mixing, i.e., homogeneity. Homogeneous mixing is especially important for generation of surface acid sites upon combination of dissimilar oxides. Of the various models to explain acid site formation in mixed oxides, one proposed by Tanabe and co-workers (1) is among the oldest and most frequently cited. They associate acidity with the "charge imbalance" that develops along a heterolinkage (*M*–O–*M′*, where *M* and *M′* are different cations) due to mismatches in cation valency and coordination number that occur when a dopant cation is placed in the matrix of a host oxide. Association of acid sites with heterolinkages provides a conceptual relationship between mixing and acidity: high acid site densities are expected of well-mixed samples. In fact, activity for reactions requiring an acid catalyst is often cited as evidence of homogeneous mixing (2, 3–5).

By providing several strategies for adjusting relative precursor reactivity (3, 7), sol–gel chemistry affords a degree of control of molecular-scale mixing that is not available with conventional preparative techniques (6, 7). We have previously compared three different chemical approaches for matching precursor reactivities—prehydrolysis of the less reactive precursor, chemical modification of the more reactive precursor, and use of a more reactive silicon precursor—for improvement of mixing in 95 mol% zirconia–5 mol% silica aerogels (3). And, using a set of titania-silica aerogels, we recently demonstrated that reactivity matching by prehydrolysis enhances component mixing at all compositions, thereby improving the acidities and catalytic activities of the calcined mixed oxides (4).

Zirconia–Silica Mixed Oxides

As a catalytic material, pure zirconia displays a wide range of properties. Its surface possesses both acidic and basic sites; it also exhibits both oxidizing and reducing characteristics (8). Zirconia has been used to support CuO for methanol synthesis (9), Rh for CO/CO_2 hydrogenation (10), and sulfate as a "solid superacid" (11, 12). Addition of small amounts of silica to form a mixed oxide stabilizes zirconia against surface area loss and crystallization upon heat treatment (3). Catalytic zirconia–silicas have been prepared by both coprecipitation (13–15) and sol–gel (3, 5, 15–17) methods. They display surface acid strengths among the highest of all oxide pairs (13, 14, 18, 19), and have been used to catalyze reactions such as alcohol dehydration (13, 14, 18), alkene isomerization (3, 5, 17), and cumene dealkyla-

[1] To whom correspondence should be addressed.

0021-9517/96 $18.00

tion (14). Many additional examples of sol–gel preparations of zirconia–silica appear in the glass literature (20–25). Incorporation of zirconia into silicate glasses is of interest because of its contribution to alkali corrosion resistance and improvement of thermal expansion properties (22–24). The sol–gel preparation is often chosen for these applications to circumvent the extraordinarily high temperatures that are necessary to prepare zirconia–silica glasses by traditional melt methods (23, 24).

In this work we apply silicon precursor prehydrolysis to preparation of zirconia–silica aerogels of three different compositions to (i) extend our work at 95 mol% zirconia–5 mol% silica to the entire composition range, (ii) demonstrate the generality of the prehydrolysis technique for enhancing mixing in sol–gel preparations of mixed oxides, and (iii) compare and contrast catalytic results with those of titania–silica for illustrating how the nature of the heterolinkages available in a mixed oxide dictates its acidic properties.

METHODS

We prepared zirconia–silica alcogels from zirconium propoxide and tetraethyl orthosilicate precursors by a method similar to that reported by Nogami and Nagasaka (21). We have documented the details of the preparation procedure elsewhere (5, 17); Table 1 summarizes the key sol–gel parameters of the samples described in this work. At each mixed oxide composition we prepared one prehydrolyzed (PH) sample in which we prereacted the silicon precursor with water to promote homogeneous component mixing and one nonprehydrolyzed (NPH) sample in which we did not. For the PH samples, we used in the prehydrolysis step a water/silicon molecular ratio (the "prehydrolysis ratio," or "PH ratio") of about 2.6 mol H_2O/mol Si, a value we recently demonstrated to promote good component mixing in preparation of 50 mol% zirconia–50 mol% silica aerogels (5, 17).

A key feature of our synthetic protocol is that, at each composition, we keep constant the overall sol–gel parameters for the PH and NPH preparations. This approach allows us to confidently isolate the effects of prehydrolysis from those of the overall parameters. However, as a result of this protocol, for our nonprehydrolyzed sample at 33 mol% zirconia–67 mol% silica we actually use a low ratio (0.6 mol H_2O/mol Si) PH preparation. At this composition, true NPH preparations having the same overall sol–gel parameters as the 2.6 mol H_2O/mol Si PH sample did not gel; instead, they formed precipitates. However, as noted in our work with 50 mol% zirconia–50 mol% silica aerogels, samples prepared with very low PH ratios are, in most respects, identical to nonprehydrolyzed materials (5, 17). To avoid confusion, when we refer to the NPH samples as a group in this paper, we mean to include the low-ratio PH 33 mol% zirconia–67 mol% silica sample.

As Table 1 shows, the overall sol–gel parameters did change with composition. As the silica content of the preparation increased, less nitric acid and more water were required to produce alcogels with target gel times between 30 s and 30 min. This range of gel times is important because

TABLE 1

Sol–Gel Parameters Used in Preparing the Zirconia–Silica Aerogels[a]

Sample ID[b]	PH water ratio (mol H_2O/mol Si)	PH acid ratio (ml HNO_3/mol Si)	Overall water ratio (mol H_2O/mol (Zr + Si))	Overall acid ratio (ml HNO_3/mol (Zr + Si))
		Prehydrolyzed (PH) mixed oxides		
AZS67-P04	2.62	6.1	2.2	14.0
AZS50-P17	2.68	6.0	2.2	10.0
AZS33-P15	2.60	4.0	4.1	4.0
		Nonprehydrolyzed (NPH) mixed oxides		
AZS67-N05	N/A[c]	N/A	2.2	14.0
AZS50-N03	N/A	N/A	2.2	10.0
AZS33-P10[d]	0.60	4.0	4.1	4.0
		Pure component oxides		
ZrO_2-9R[e]	N/A	N/A	2.0	52.0
SiO_2-27[f]	N/A	N/A	4.0	9.5

[a] Precursor concentration held constant at 1.0 mmol (Zr + Si)/ml PrOH for all mixed oxide preparations.

[b] Mixed oxide nomenclature: AZSxx = zirconia–silica aerogel containing xx mol% zirconia; Pyy = silicon precursor prehydrolysis, batch number yy; Nzz = no silicon precursor prehydrolysis, batch zz.

[c] Not applicable.

[d] Strictly not a NPH sample; see text for explanation.

[e] See reference (42) for details of silica preparation.

[f] See reference (28) for details of zirconia preparation.

it delivers alcogels having the structural rigidity required for the subsequent supercritical drying step. The shift to lower nitric acid amounts and higher water ratios is necessary to increase reaction rates in compensation for the low reactivity of the silicon precursor.

After drying by contact with flowing supercritical CO_2, the product aerogels were ground to <100 mesh and vacuum dried at 383 K and then 523 K for removal of moisture and residual organics. Vacuum-dried samples were calcined for 2 h at 773 K in flowing oxygen. Most of our characterization work was performed on the calcined samples.

We have described in detail the techniques used to characterize our samples elsewhere (3, 4, 17). A brief summary of the key methods follows. The activities of calcined samples as catalysts for 1-butene isomerization, a reaction requiring a weak Brønsted acid catalyst (26), were measured as reaction rate (*cis*- and *trans*-2-butene reaction products) on a per area basis at standard conditions (95 sccm helium, 5 sccm 1-butene, 423 K, 1 atm, ~0.2 g sample, and 95 min time on stream). Total acid site densities of the calcined samples were estimated from the results of ammonia TPD experiments performed at conditions selected to simulate those used for the isomerization trials (NH_3 adsorption at 423 K, desorption between 423 and 773 K at 10 K/min). Diffuse reflectance infrared Fourier transform (DRIFT) spectroscopy was used to characterize the hydroxyl inventory (~2800–3800 cm^{-1}) and the skeletal vibration region (~600–1300 cm^{-1}) of the calcined aerogels. After collection of the "clean" DRIFT spectrum, the sample was exposed to pyridine and a second spectrum was collected for estimation of relative Lewis and Brønsted acid site populations by the method of Basila and Kantner (27). DRIFT experiments were also performed at conditions simulating those used for isomerization activity testing (423 K in a flowing helium atmosphere).

Samples vacuum dried at 523 K were analyzed by DTA (differential thermal analysis) to estimate the temperature at which the zirconia component crystallized into its metastable tetragonal form (28). Surface areas of aerogels calcined at 773 K were determined from nitrogen adsorption/desorption experiments analyzed by the BET method.

RESULTS

Acidic/Catalytic Properties

Figure 1 illustrates how the activities of the mixed oxides as catalysts for 1-butene isomerization vary as functions of composition and preparation method. Unlike the pure component oxides, which are both inactive, the mixed oxides display considerable activity for isomerization, suggesting formation of at least Brønsted acid sites upon combination of the components. Note also that at each mixed oxide composition, the prehydrolyzed sample is more active than its nonprehydrolyzed counterpart. As we recently reported,

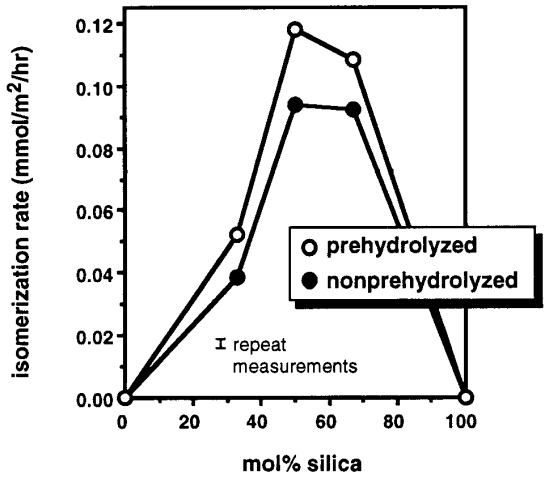

FIG. 1. Activities of zirconia–silica aerogels as catalysts for isomerization of 1-butene, reported as reaction rate per unit area at standard conditions (see text). Error bar shows range of back-to-back activity measurements. All samples calcined at 773 K in oxygen for 2 h prior to activity testing.

prehydrolysis improves isomerization activities of 50 mol% zirconia–50 mol% silica (5, 17), 95 mol% zirconia–5 mol% silica (3), and titania–silica aerogels (4). In all cases, we have attributed the higher activity of the prehydrolyzed samples to better molecular-scale mixing of the oxide components.

The isomerization activities of our samples are, of course, related to the number and type of surface acid sites that they posses. Figure 2 shows how the acidities of the prehydrolyzed (PH) samples vary as a function of composition. The total heights of the bars in Fig. 2 represent their total

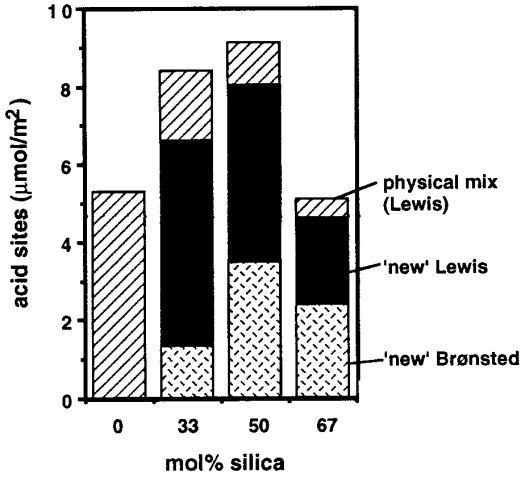

FIG. 2. Acid site distributions of zirconia–silica aerogels. Total acidity estimated from ammonia TPD experiments (adsorption at 423 K, desorption between 423 and 773 K); Lewis/Brønsted ratio estimated from DRIFT spectrum of adsorbed pyridine at 423 K. All samples originally calcined at 773 K in oxygen for 2 h.

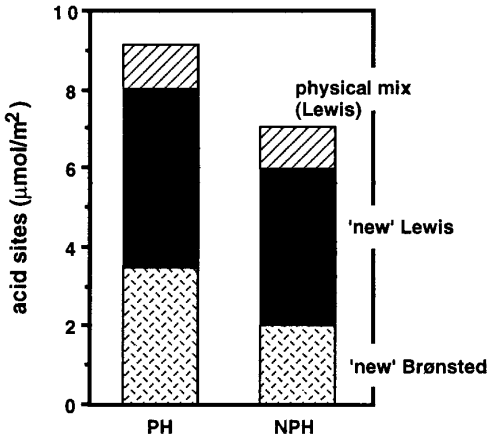

FIG. 3. Acid site distributions of the prehydrolyzed (PH) and nonprehydrolyzed (NPH) 50 mol % zirconia–50 mol% silica aerogels. Both samples originally calcined at 773 K in oxygen for 2 h.

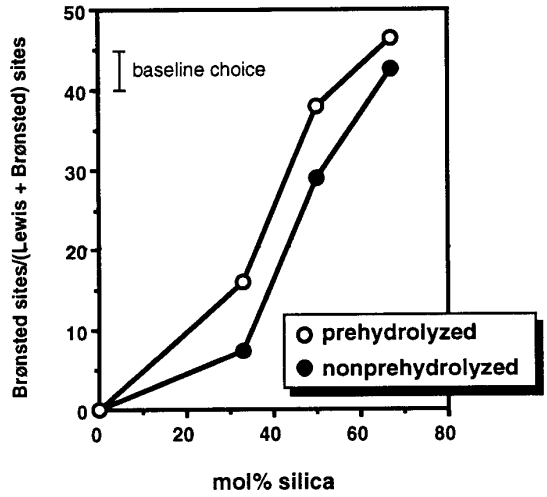

FIG. 4. Fractional Brønsted population, defined as Brønsted sites/[Lewis sites + Brønsted sites], as a function of composition of zirconia–silica aerogels. Lewis/Brønsted ratio estimated from DRIFT spectrum of adsorbed pyridine at 423 K. Error bar shows effect of baseline choice (for integration of peak intensities; see Ref. (5) for details) on results. All samples originally calcined at 773 K in oxygen for 2 h.

acid site densities as measured by ammonia TPD. Maximum acidity, 9.1 μmol/m^2, occurs at a 50 mol% zirconia–50 mol% silica composition. We have further classified the total acid site populations of our aerogels in the following manner. First, we used the DRIFT spectra of pyridine adsorbed on the samples as a basis for estimating the relative populations of Lewis and Brønsted sites. Then, we separated that portion of the Lewis site population that could be expected simply from a physical mixture of the two calcined pure components. (Our DRIFT data show that zirconia aerogel possesses exclusively Lewis sites. Since silica is well known not to be acidic (14, 29), we did not characterize the pure component aerogel by ammonia TPD. As expected, silica aerogel adsorbed no pyridine during the DRIFT experiments.) As Fig. 2 illustrates, significant populations of "new" acid sites form at all mixed oxide compositions, an indication that acidic Zr–O–Si linkages are present in those samples.

It is also significant that the new sites formed by component oxide mixing in the 67 mol% zirconia–33 mol% silica sample are predominantly *Lewis*. At higher silica contents, however, new sites are increasingly likely to be *Brønsted*. As we will discuss later, these observations are consistent with the Tanabe model which predicts Lewis site formation at zirconia-rich compositions and Brønsted site formation in silica-rich environments. Also note that, as expected, Brønsted site densities (Fig. 2) correlate reasonably well with isomerization activities (Fig. 1).

Figure 3 illustrates the differences between PH and NPH acid site populations for the 50 mol% zirconia–50 mol% silica samples. Total site density is higher in the prehydrolyzed sample, providing supporting evidence of its superior degree of component mixing. The PH preparation also tends to favor formation of Brønsted sites. Indeed, as shown in Fig. 4, prehydrolyzed samples display higher fractional Brønsted acidities over the entire composition range.

As we described previously, silicon precursor prehydrolysis also enhances both total acid site density and fractional Brønsted population in titania–silica aerogels (4).

Figure 5 shows the hydroxyl region of the IR spectra, collected at 1-butene isomerization conditions, as a function of composition for the prehydrolyzed samples and the pure component oxides. Zirconia aerogel and the 67 mol% zirconia–33 mol% silica mixed oxide have very low hydroxyl contents, consistent with the predominance of Lewis

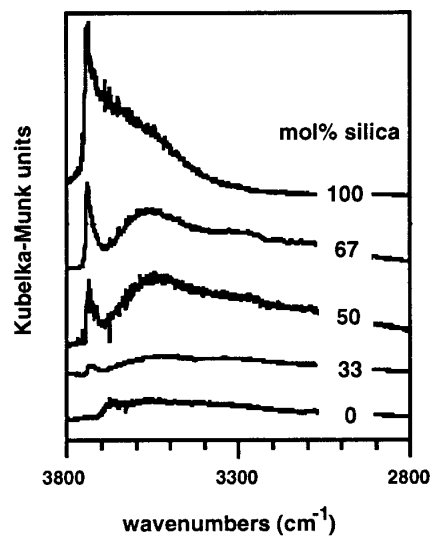

FIG. 5. Hydroxyl region DRIFT spectra of the prehydrolyzed mixed zirconia–silica and pure component aerogels. Spectra collected at 423 K in flowing helium. All samples originally calcined at 773 K in oxygen for 2 h.

acid sites in those samples (see Fig. 4). All mixed oxides display both a high frequency "spike" (~3740 cm^{-1}), characteristic of the stretch of "isolated" SiO–H (7, 30) and a broader low wavenumber feature, related to hydrogen bonding among neighboring OH groups (7, 30). Both features grow as silica content—and fractional Brønsted acidity (see Fig. 4)—increase. At the highest silica contents, the high wavenumber spike clearly dominates.

Textural/Structural Properties

The response of the aerogels' surface areas to composition and preparation method is shown in Fig. 6. Compared to the prehydrolyzed samples, nonprehydrolyzed samples have slightly larger surface areas. This result is consistent with our previous reports of surface area stabilization by "silica-rich surface patches" that is characteristic of zirconia–silicas prepared without silicon precursor prehydrolysis (3, 5).

The skeletal regions of the DRIFT spectra of our prehydrolyzed samples and the pure component aerogels appear in Fig. 7. In the spectrum of pure silica aerogel, four features are observed: asymmetric Si–O–Si "network" stretches at 1080 and 1180 cm^{-1}, the corresponding symmetric stretch at 810 cm^{-1}, and Si–O^- or Si–OH at 980 cm^{-1} (13, 14, 22, 23). In the 67 mol% silica–33 mol% zirconia mixed aerogel, the 810 and 980 cm^{-1} features disappear, the 1180 cm^{-1} shoulder becomes part of the "main" 1080 cm^{-1} feature, and the 1080 cm^{-1} peak shifts to lower wavenumber. The main Si–O–Si feature continues to move toward increasingly lower wavenumbers as the zirconia content of the mixed oxide rises. These spectral changes are consistent with a weakening of the silica network by zirconium atoms; other researchers have reported similar trends in the IR spectra of their catalytic zirconia–silicas (13, 14).

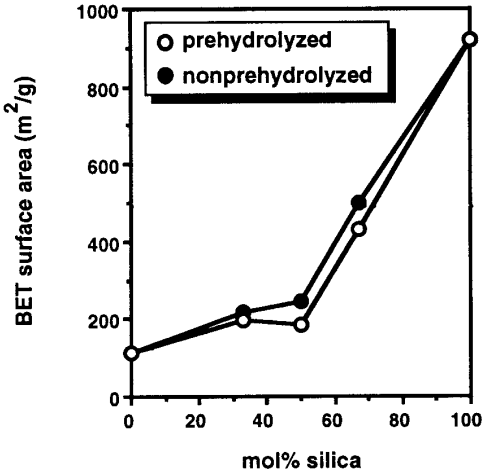

FIG. 6. BET surface areas of zirconia–silica aerogels as functions of composition and preparation method. All samples originally calcined at 773 K in oxygen for 2 h.

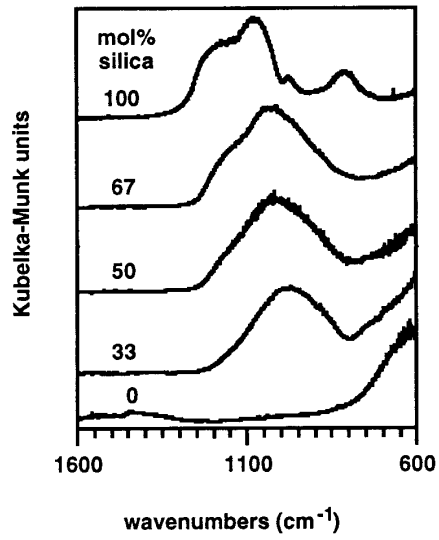

FIG. 7. Skeletal vibration region DRIFT spectra of the prehydrolyzed mixed zirconia–silica and pure component aerogels. Spectra collected at 423 K in flowing helium. All samples originally calcined at 773 K in oxygen for 2 h.

Addition of even small amounts of silica to zirconia is well known to stabilize zirconia in an X-ray amorphous form, thereby delaying crystallization to its metastable tetragonal phase to higher heat treatment temperatures (3, 16). In Table 2, we use DTA data to illustrate the effects of both composition and preparation method on zirconia's crystallization. At each mixed oxide composition, the temperature range of crystallization is consistent with literature reports for both zirconia–silica catalysts (14, 15) and glasses (24, 25, 31–34). Note that the well-mixed, prehydrolyzed samples stabilize amorphous zirconia to higher temperatures

TABLE 2

Temperature of Zirconia's Crystallization in the Mixed Aerogels[a]

Composition (mol% silica)	Preparation type (PH/NPH)	DTA peak location[b] (K)
0	N/A[c]	753
33	NPH	1081
33	PH	1101
50	NPH	1149
50	PH	1170
67	NPH	—[d]
67	PH	—[d]

[a] Differential thermal analysis (DTA) performed on mixed oxides vacuum dried at 523 K, zirconia dried at 383 K.

[b] Exothermic peak in temperature region in which the zirconia component crystallizes into its metastable tetragonal form as confirmed by independent X-ray diffraction experiments (5, 28).

[c] Not applicable.

[d] No feature detected below 1273 K.

than do their nonprehydrolyzed counterparts. In our work with 50 mol% zirconia–50 mol% silica aerogels, we have attributed this effect to the ability of the siloxane network that spans prehydrolyzed samples to immobilize zirconium atoms through attachments at Zr–O–Si linkages (5).

DISCUSSION

Homogeneity of Catalytic Zirconia–Silicas Prepared by Other Methods

In this work, as well as in our previous reports of zirconia–silica aerogels (3, 5), we have identified several characteristics of zirconia–silicas that are, at least in a relative sense, molecularly well-mixed. Foremost among these characteristics are high acidity/catalytic activity and the delay of the zirconia component's crystallization to higher heat-treatment temperatures. Measurements of these properties have been reported in the literature for catalytic zirconia–silicas prepared by a variety of methods. In this section, we use these examples to illustrate the "range of homogeneity" that can be accessed by the various techniques.

Table 3 summarizes several author's recent reports of zirconia–silica surface area, acidity (ammonia adsorption techniques), and crystalline state; we have chosen to show data at two compositions to maximize overlap among some very disparate reports. Listed at the top of the table are our samples described in this paper. They are followed by coprecipitates of Bosman *et al.* (13) that were prepared from H_2SiF_6 and H_2ZrF_6 precursors chosen specifically to promote good mixing through minimization of precipitation rate differences. Toba *et al.* reported results for samples made by three different methods (15). The first is a sol–gel preparation using zirconium *n*-propoxide and tetraethylorthosilicate precursors in the presence of a "complexing agent" (hexylene glycol). The complexing agent is used to control reaction rates for enhancement of component mixing. From the same precursor pair, they also prepared a set of "conventional" coprecipitates. For their third sample set, they kneaded the wet hydrogels of the separately precipitated precursors. Sohn and Jang (14) described materials coprecipitated from zirconium oxychloride and sodium silicate.

Because of differences in the details of the ammonia adsorption techniques used by the various authors as well as differences among their choices of a "standard" calcination temperature, meaningful conclusions might have been difficult to draw from comparisons of site density data. However, the size of acidity difference that separates our samples and those of Bosman *et al.* from the Toba *et al.* and Sohn and Jang materials—a full order of magnitude—suggests that a real difference exists between the former and latter pairs. (We note that, while the differences become smaller,

TABLE 3

Comparison of Literature Reports of Zirconia–Silicas Prepared by Different Methods

Reference/ sample type	Composition (mol% silica)	Surface area (m^2/g, temp.[a])	Acidity (μmol/m^2, temp.[a])	Comments
This work	67	430, 773 K	5.1, 773 K	
(PH)	50	186, 773 K	9.1, 773 K	Crystallizes at ~1170 K[c]
This work	67	498, 773 K	N/A[b]	
(NPH)	50	244, 773 K	7.0, 773 K	Crystallizes at ~1149 K[c]
Bosman *et al.* (13)	75	131, 773 K	8.2, 573 K	XPS[d] shows surface
co-ppt.w/flourinated	50	42, 773 K	6.4, 573 K	segregation of silica
precursors				
Toba *et al.* (15)	83	~400, 823 K	~0.77, 823 K	Last to crystallize[e] in this group;
sol–gel/complex'n	50	~250, 823 K	N/A	best mixed by NMR
Toba *et al.* (15)	83	~390, 823 K	~0.77, 823 K	Second to crystallize in this group;
coprecipitate	50	<50, 823 K	N/A	second best mixed by NMR
Toba *et al.* (15)	83	~320, 823 K	~0.74, 823 K	First to crystallize in this group;
kneaded hydrogels	50	<50, 823 K	N/A	poorest mixing by NMR
Sohn and Jang (14)	83	507, 673 K	~0.60, 673 K	
coprecipitates	48	280, 673 K	~0.50, 673 K	

[a] Calcination temperature.
[b] Not available.
[c] Estimated from results of differential thermal analysis (see text).
[d] XPS = X-ray photoelectron spectroscopy.
[e] Based on results of X-ray diffraction experiments.

the acidity "rank order" remains the same when viewed on a "sites per mass" basis.) Since high acid site densities are characteristic of well-mixed samples, we conclude that silicon precursor prehydrolysis and the Bosman *et al.* (13) strategy of precipitation with fluorinated precursors are more effective for promoting homogeneous molecular-scale mixing than any of the methods used by Toba *et al.* (15) or Sohn and Jang's (14) traditional coprecipitation procedure.

The high degree of mixing that we infer for the Bosman *et al.* (13) materials is of particular interest because XPS (X-ray photoelectron spectroscopy) analysis suggests that they are partially segregated, having silica located preferentially at their surfaces. This observation underscores two important points: (i) the acidity scale for ranking homogeneity is a *relative* one and (ii) "perfect" molecular scale mixing was probably not achieved by even the most effective of the techniques cited in the table. The Bosman *et al.* (13) samples also have among the lowest surface areas of the zirconia–silicas shown in the table. Thus, the aerogel preparation is unique in its ability to deliver materials having both high surface area and high acid site density. We also note that, while not as well mixed as their prehydrolyzed counterparts, our nonprehydrolyzed aerogels appear to be much better mixed than materials prepared by conventional coprecipitation methods.

The trio of methods used by Toba *et al.* (15) also contributes to our understanding of homogeneity in catalytic zirconia–silicas. As illustrated in Table 3, acidity data suggest that the degree of mixing achievable by these techniques is similar. However, solid state ^{29}Si NMR results clearly demonstrate a rank order of mixing within the three methods: sol–gel (best mixing) > coprecipitation > hydrogel kneading. In addition, their X-ray diffraction data are consistent with the relationship that we observed between good mixing and the delay of zirconia's crystallization to higher temperature: the kneaded hydrogel crystallizes at the lowest temperature, followed by the coprecipitate, and finally by the sol–gel material.

While it does provide a small mixing improvement over coprecipitated and kneaded materials, Toba *et al.*'s complexing agent assisted sol–gel technique delivers samples that, based on acidity evidence, are not nearly as well mixed as our aerogels or Bosman *et al.*'s zirconia–silicas (13). We view this as an unexpected result because use of a complexing agent, like silicon precursor prehydrolysis and coprecipitation of fluorinated precursors, is a technique designed specifically to overcome precursor reactivity differences for promoting homogeneous mixing. While we cannot offer an explanation for their complexing agent sample's low acidity, we note that the synthetic approach appears to be sound. We recently reported, for example, our application of a related method, known as "chemical modification," to successfully prepare a well-mixed 95 mol% zirconia–5 mol% silica aerogel (3).

Comparison with Titania–Silica

The responses of the acidic properties of zirconia–silica aerogels to silicon precursor prehydrolysis, including higher acid site densities, fractional Brønsted populations, and 1-butene isomerization activities completely parallel those we have previously reported for the titania–silica system (4). The similarity between the two oxide pairs convincingly demonstrates the general validity and applicability of the prehydrolysis technique in particular and precursor reactivity matching in general for promoting homogeneous mixing in sol–gel preparation of two-component oxides.

Several important differences do exist between the two mixed oxide pairs, however. Most can be illustrated by comparing the shapes of their respective isomerization activity plots. In Fig. 8 we combine the data from Fig. 1 and our previously published results of titania–silica aerogel activities (4). We note three significant differences: (i) zirconia–silica's maximum activity occurs at higher silica content, (ii) the difference between well-mixed (PH) and poorly-mixed (NPH) samples is considerably larger in titania–silica, and (iii) the absolute range of activity is higher in zirconia–silica. Within the framework of the Tanabe acidity model (1), these differences can be related to the types and numbers of heterolinkages (M–O–Si; M = Ti, Zr) that form in the two systems.

The central feature of the Tanabe model is the calculation of "excess charge" at the site of the minor component cation (1). The basis for the calculation is a hypothetical heterolinkage in which cations retain their pure-component coordinations while oxygen atoms adopt the coordination of oxygens in the major pure component. This linkage can be viewed as the preferred local M–O–

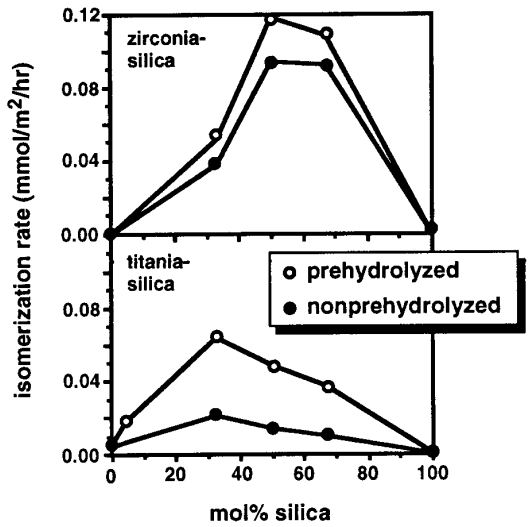

FIG. 8. Comparison of the 1-butene isomerization activities of zirconia–silica (top panel) and titania–silica (bottom panel) aerogels. All samples originally calcined at 773 K in oxygen for 2 h.

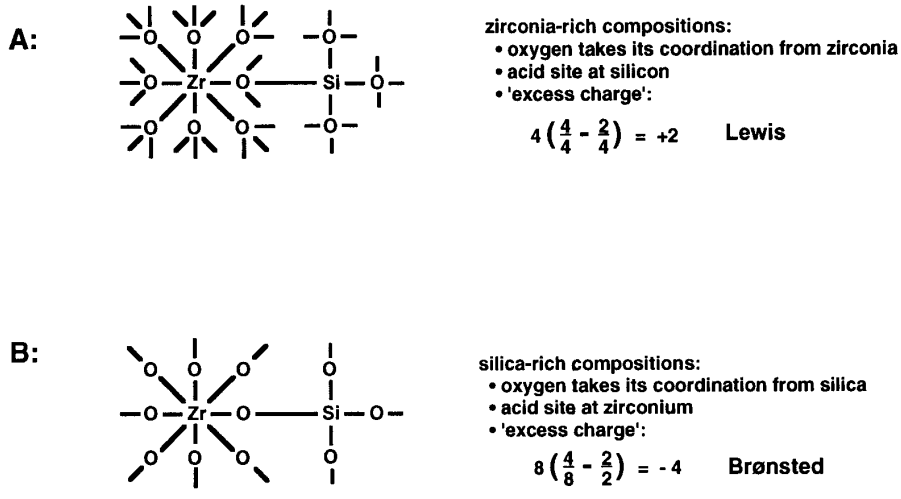

FIG. 9. Excess charge calculations, following the Tanabe model, for zirconia–silica heterolinkages: (a) model's prediction for zirconia-rich compositions, (b) model's prediction for silica-rich compositions.

M' atomic configuration in the composition range under consideration; it will typically coexist with one or more minor linkages, especially at intermediate compositions. Excess charge is computed by distributing the formal charges of both the minor cation and its nearest-neighbor oxygens among all the bonds in which they participate. Excess negative charge is balanced by protons to form a Brønsted acid site. Positive excess charge, which is presumably balanced by negative charges distributed elsewhere in the mixed oxide matrix, is associated with a Lewis site.

As illustrated in Fig. 9, application of the model to zirconia–silica predicts formation of Lewis acid sites at zirconia-rich compositions and Brønsted sites in the silica-rich region. These results compare very well with our experimental observations: recall that new acid sites were predominantly Lewis at low silica content, but were increasingly likely to be Brønsted as silica content increased. These trends are also reflected in the 1-butene isomerization activities of our zirconia–silicas: as shown in Figs. 1 and 8, a broad activity maximum occurs in the range of 50 to 67 mol% silica. Our data also clearly illustrate that both Brønsted and Lewis sites exist at all mixed oxide compositions (Fig. 2), an indication that more than one—most likely several—types of heterolinkages coexist. This is not a surprising result; we expect a family of different heterolinkages to be present in samples with local variations in the goodness of molecular-scale mixing. However, it is most important to note that despite this complication, this very simple model properly predicts the *trends* in acid site type as composition changes.

As shown in Figs. 10A and 10B, application of the Tanabe model to titania–silica predicts a preference for Lewis sites in the titania-rich region and Brønsted sites at silica-rich compositions; this result parallels the zirconia–silica case (Fig. 9). However, the assignment of octahedral coordination to titanium cations in silica-rich environments is incorrect. As we described in our previous report of titania–silica aerogels, the glass literature teaches that titanium cations can isomorphically substitute for silicon in the silica matrix, thereby adopting silicon's tetrahedral coordination (4). Indeed, titanium can enter the silica matrix *exclusively* in the tetrahedral coordination up to about 8 mol% (35). Titanium's ability to enter the network in this manner is linked to many desirable properties in multicomponent glass preparation (35).

However, from a catalytic—especially acidic—perspective, tetrahedral coordination of titanium has very different implications. As illustrated in Fig. 10C, a heterolinkage containing a tetrahedrally coordinated titanium cation lacks the charge imbalance required by the model to create a Brønsted acid site. Coordinative unsaturation at the tetrahedrally coordinated titanium cation can, in fact, contribute to Lewis acidity (36). Since Brønsted sites are not favored at either composition extreme (Figs. 10A and 10C), maximum 1-butene isomerization activity is no longer restricted to any subset of the composition range as it was in the zirconia–silica system. As Fig. 8 shows, maximum activity is observed at 33 mol% silica–67 mol% titania. At such titania-rich compositions, the Tanabe model predicts that Lewis acid sites should be favored (Fig. 10A). Consistent with this prediction, we have observed that Lewis acidity is the dominant form in our 33 mol% silica–67 mol% titania aerogels (4). We infer, therefore, that maximum 1-butene isomerization occurs at 33 mol% silica because *minor* linkages having Brønsted character—the linkage shown in Fig. 10B is one possible example—are most populous at that composition. (Our association of Brønsted acidity with minor linkages in titania–silica differs from another recent report (4); it represents an evolutionary improvement in our understanding of the titania–silica system.) We note

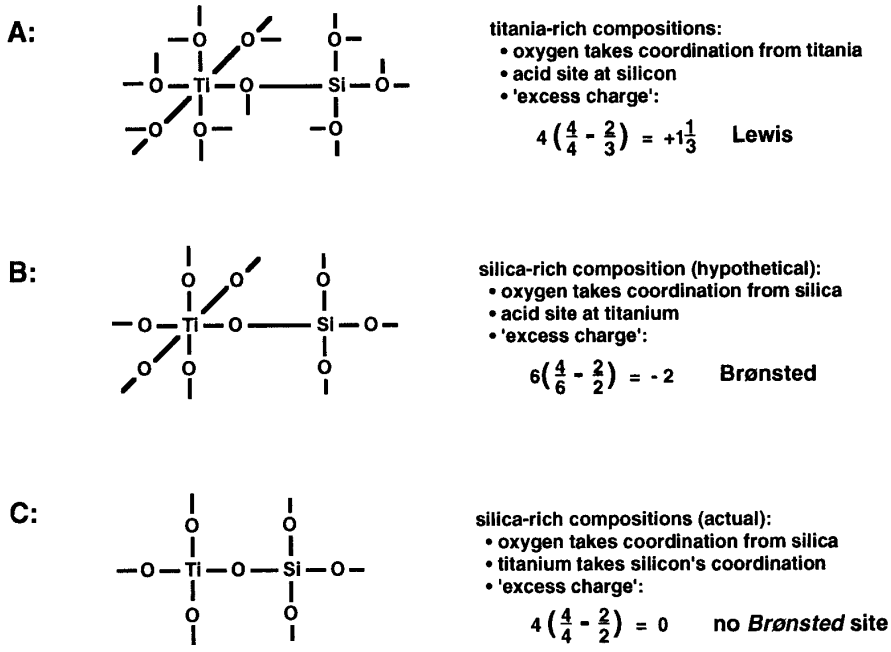

FIG. 10. Excess charge calculations, following the Tanabe model, for titania–silica heterolinkages: (a) model's prediction for titania-rich compositions, (b) model's prediction for silica-rich compositions, (c) application to actual linkage in silica-rich environment.

that titanium's ability to adopt tetrahedral coordination is the essence of the contrasting behaviors of titania–silica and zirconia–silica: zirconium does not enter the silica network in tetrahedral coordination at any composition (37), preferring coordinations of 6 (38), 7 (37), or 8 (21).

Our application of the Tanabe model to both zirconia–silica and titania–silica illustrates both its strengths and its weaknesses. Given accurate knowledge of atomic coordinations, the conceptually simple "excess charge" calculation successfully predicts many of the acidic trends in mixed oxide catalytic materials. However, the model's rules for assigning heterolinkage coordination numbers lack the same general applicability. We suspect, in fact, that many of the reported instances in which the prediction of the model conflicts with experimental results (1) may be attributable to deficiencies in coordination assignments, not the excess charge calculation.

Comparison of the skeletal vibration regions of the zirconia–silica and titania–silica DRIFT spectra uncovers an interesting difference that may also be related to transition metal coordinations. In Fig. 11, we compare the spectrum of our prehydrolyzed 50 mol% zirconia–50 mol% silica (previously appearing as the middle spectrum in Fig. 7) to that of the corresponding 50 mol% titania–50 mol% silica sample (A-TS57wt #5 in Ref. (4)). As described earlier, zirconia–silica displays a single feature in the 800–1300 cm^{-1} region; it is assigned to a Si–O–Si network asymmetric stretch. In contrast, the spectrum of titania–silica contains a second feature near 930 cm^{-1}. Zhu *et al.* have observed a similar difference between the spectra of zirconia–silica and titania–silica (22). The 930 cm^{-1} feature has been assigned to both (i) vibrations of Si–O–Ti bonds in which titanium is tetrahedrally coordinated and (ii) an $Si–O^-$ stretch (4). Even though we cannot make a definitive assignment, we note that, should (i) be correct, the absence of a corresponding feature in the zirconia–silica spectrum supports the uniqueness of tetrahedrally coordinated transition metal cations to titania–silica.

Figure 8 also illustrates that the activity enhancement attributable to prehydrolysis is considerably larger in titania–

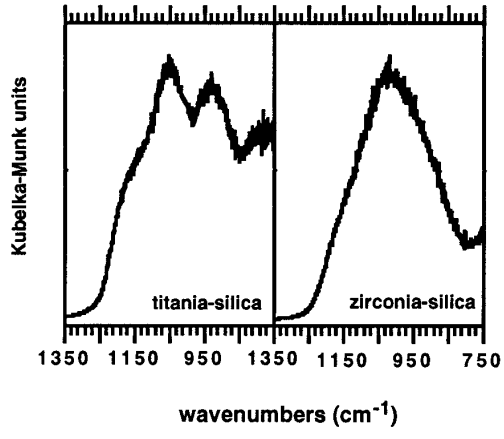

FIG. 11. Comparison of skeletal vibration region DRIFT spectra of 50 mol% titania–50 mol% silica (left panel) and 50 mol% zirconia–50 mol% silica (right panel) aerogels. Spectra collected at 423 K in flowing helium. Both samples originally calcined at 773 K in oxygen for 2 h.

silica than in zirconia–silica. This difference could be due to the fact that we are probing different ranges of absolute mixing in the two cases. We use a higher prehydrolysis ratio in the titania–silica set (4.0 vs 2.6 mol H_2O/mol Si) and, as we have shown in our work with 50 mol% zirconia–50 mol% silica aerogels, additional mixing improvements can be made as the ratio is increased beyond 2.6 mol/mol (5).

Also of interest is the difference in absolute 1-butene isomerization activities between zirconia–silica and titania–silica. At its maximum, zirconia–silica is about twice as active as the most active titania–silica. One possible explanation for this difference could be higher Brønsted site densities in zirconia–silica. Recall that zirconia–silica's Brønsted sites form at preferred (more populous) heterolinkages. In titania–silica, on the other hand, Brønsted acidity arises from minor (less populous) linkages. We also note that, while the zirconium and titanium have similar electronegativities (39), coordination differences between titanium and zirconium reflect themselves as a greater degree of charge imbalance in zirconia–silica when viewed from the perspective of the Tanabe model (compare Figs. 9 and 10), suggesting that the zirconia–silica sites could be, in some manner, stronger. Selected examples of both our titania–silicas and zirconia–silicas have been examined by a potentiometric titration technique that provides estimates of the strength distributions of Brønsted acid sites (40). Consistent with the charge imbalance difference, isomerization activity correlates with stronger sites in zirconia–silica than in titania–silica (41). In addition, turnover frequencies at the strong zirconia–silica sites appears to be about an order of magnitude higher than in titania–silica (41).

CONCLUSIONS

Zirconia–silica aerogels prepared by prehydrolysis of the silicon precursor display improved acidity, higher fractional Brønsted content, and higher activity as catalysts for 1-butene isomerization than do the corresponding nonprehydrolyzed materials. These observations reinforce a link that we have previously reported between prehydrolysis and homogeneous component mixing during preparation of silica-containing mixed oxide aerogels. Specifically, parallels between the response of zirconia–silica and titania–silica to silicon precursor prehydrolysis demonstrate the general applicability of the prehydrolysis technique in particular and of precursor reactivity matching in general for promoting homogeneous mixing in sol–gel preparations of two-component oxides. In addition, based on comparisons with literature reports of acid site densities of zirconia–silicas prepared by a variety of methods, we conclude that our aerogel preparation, even in its nonprehydrolyzed form, delivers materials that are among the most homogeneously mixed.

Zirconia–silica and titania–silica also display some important contrasting behaviors. At silica-rich compositions, titanium adopts silica's tetrahedral coordination; zirconium does not. This fundamental difference between the two mixed oxide pairs has important implications for catalytic properties, including the manner in which 1-butene isomerization activity responds to composition variations.

Comparison of titania–silica to zirconia–silica also provides insight into the Tanabe model of mixed oxide acidity. As clearly demonstrated by the titania–silica example, the weakness of the model rests with its rules for assigning atomic coordinations in the mixed oxide's heterolinkages. However, when coordinations are estimated with reasonable accuracy, as is the case for zirconia–silica, the model's calculation of excess charge appears to be a simple and powerful predictor of both acidity development and acid site type. Our success in using sol–gel chemistry to explore these issues demonstrates its key role in understanding of catalytic phenomena.

ACKNOWLEDGMENTS

This work is supported by the Division of Chemical Sciences, Office of Basic Energy Sciences, Office of Energy Research, U.S. Department of Energy (Grant DE-FG02-93ER14345).

REFERENCES

1. Tanabe, K., Sumiyoshi, T., Shibata, K., Kiyoura, T., and Kitagawa, J., *Bull. Chem. Soc. Jpn.* **47**(5), 1064 (1974).
2. Tanabe, K., Itoh, M., Morishige, K., and Hattori, H., *in* "Preparation of Catalysts" (B. Delmon, P. A. Jacobs, and G. Poncelet, Eds.), p. 65. Elsevier, Amsterdam, 1976.
3. Miller, J. B., Rankin, S. E., and Ko, E. I., *J. Catal.* **148**, 673 (1994).
4. Miller, J. B., Johnston, S. T., and Ko, E. I., *J. Catal.* **150**, 311 (1994).
5. Miller, J. B., and Ko, E. I., "Advanced Techniques in Catalyst Preparations." Preprints to American Chemical Society Meeting, Anaheim, 1995.
6. Courty, P., and Marcilly, C., *in* "Preparation of Catalysts" (B. Delmon, P. A. Jacobs, and G. Poncelet, Eds.), p. 119. Elsevier, Amsterdam, 1976.
7. Brinker, C., and Scherer, G., "Sol-Gel Science: The Physics and Chemistry of Sol-Gel Processing." Academic Press, Boston, 1990.
8. Tanabe, K., *Mater. Chem. Phys.* **13**, 347 (1985).
9. Amenomiya, Y., *Appl. Catal.* **30**, 57 (1987).
10. Iizuka, T., Tanaka, Y., and Tanabe, K., *J. Catal.* **76**, 1 (1982).
11. Hino, M., and Arata, K., *J. Chem. Soc. Chem. Commun.* 851 (1980).
12. Ward, D. A., and Ko, E. I., *J. Catal.* **150**, 18 (1994).
13. Bosman, H. J. M., Kruissink, E. C., van der Spoel, J., and van den Brink, F., *J. Catal.* **148**, 660 (1994).
14. Sohn, J. R., and Jang, H. J., *J. Mol. Catal.* **64**, 349 (1991).
15. Toba, M., Mizukami, F., Niwa, S., Sano, T., Maeda, K., Annila, M., and Komppa, V., *J. Mol. Catal.* **94**, 85 (1994).
16. Soled, S., and McVicker, G. B., *Catal. Today* **14**, 189 (1992).
17. Miller, J. B., and Ko, E. I., *J. Catal.* **153**, 194 (1995).
18. Dzisko, V., *in* "Proceedings, 3rd International Congress on Catalysis, Amsterdam, 1964." Wiley, New York, 1965.
19. Shibata, K., Kiyoura, T., Kitagawa, J., Sumiyoshi, T., and Tanabe, K., *Bull. Chem. Soc. Jpn.* **46**, 2985 (1973).
20. Lee, S., and Condrate, R., *J. Mater. Sci.* **23**(8), 2951 (1988).
21. Nogami, M., and Nagasaka, K., *J. Non-Cryst. Solids* **109**, 79 (1989).
22. Zhu, C., Hou, L., Gan, F., and Jiang, Z., *J. Non-Cryst. Solids* **63**, 105 (1984).
23. Nogami, M., *J. Non-Cryst. Solids* **69**, 415 (1985).
24. Li., X., and Johnson, P., *Mater. Res. Soc. Proc.* **180**, 355 (1990).

25. Nogami, M., and Tomozawa, M., *J. Am. Ceram. Soc.* **69**(2), 99 (1986).
26. Goldwasser, J., Engelhardt, J., and Hall, W. K., *J. Catal.* **71**, 381 (1981).
27. Basila, M. R., and Kantner, T. R., *J. Phys. Chem.* **70**, 1681 (1966).
28. Ward, D. A., and Ko, E. I., *Chem. Mater.* **5**(7), 956 (1993).
29. Liu, Z., Tabora, J., and Davis, R. J., *J. Catal.* **149**, 117 (1994).
30. Little, L. H., "Infrared Spectra of Adsorbed Species." p. 230. Academic, London, 1966.
31. Kamiya, K., Sakka, S., and Tatemichi, Y., *J. Mater. Sci.* **15**, 1765 (1980).
32. Campaniello, J., Rabinovich, E., Berthet, P., Revcolevschi, A., and Kopylov, N., *Mater. Res. Soc. Symp. Proc.* **180**, 541 (1990).
33. Monros, G., Marti, M., Carda, J., Tena, M., Escribano, P., and Anglada, M., *J. Mater. Sci.* **28**, 5852 (1993).
34. Miranda Salvado, I., Serna, C., and Fernandez Navarro, J., *J. Non-Cryst. Solids* **100**, 330 (1988).
35. Evans, D., *J. Non-Cryst. Solids* **52**, 115 (1981).
36. Imamura, S., Nakai, T., Kanai, H., and Ito, T., *Catal. Lett.* **28**, 277 (1994).
37. Bihuniak, P., and Condrate, R., *J. Non-Cryst. Solids* **44**, 331 (1981).
38. Osuka, T., Morikawa, H., Marumo, F., Tohji, K., Udagawa, Y., Yasumori, A., and Yamane, M., *J. Non-Cryst. Solids* **82**, 154 (1986).
39. Pauling, L., "The Chemical Bond." Cornell Univ. Press. Ithaca, New York, 1967.
40. Contescu, C., Jagiello, J., and Schwarz, J. A., *Langmuir* **9**, 1754 (1993).
41. Contescu, C., Popa, V. T., Miller, J. B., Ko, E. I., and Schwarz, J. A., *J. Catal.* **157**, 244 (1995).
42. Maurer, S. M., Ph.D. Thesis, Carnegie Mellon University, 1991.